ISSN: 0975-833X

Available online at http://www.journalcra.com

International Journal of Current Research
Vol. 11, Issue, 04, pp.3199-3205, April, 2019

DOI: https://doi.org/10.24941/ijcr.35003.04.2019

INTERNATIONAL JOURNAL OF CURRENT RESEARCH

RESEARCH ARTICLE

PHOTOSENSITIZATION, PHOTOCATALYSIS AND PHOTO FENTON REACTIONS OF HEMIN ANCHORED $SrTiO_3$ / SnO_2 COMPOSITE FOR THE DEGRADATION OF RHODAMINE B: A COMPARATIVE STUDY WITH PRISTINE $SrTiO_3$ AND SnO_2

***Gomathi Devi, L., Anitha, B.G. and Shyamala, R.**

Department of Post Graduate Studies in Chemistry, Central College City Campus, Dr. Ambedkar Street, Bangalore University, Bangalore 560001, India

ARTICLE INFO

Article History:
Received 12th January, 2019
Received in revised form
09th February, 2019
Accepted 16th March, 2019
Published online 30th April, 2019

Key Words:
Photosensitization, Inter System Crossing, Photo-Fenton process, Photocatalysis.

ABSTRACT

In the present study anchoring of hemin a protoporphyrin IX Fe (III) molecule on the surface of $SrTiO_3/SnO_2$ composite (H-(STO / SnO_2)) is attempted. STO / SnO_2 composite show activity under visible light due to the staggering band edge positions. However the activity under solar light is very poor. When hemin is anchored on the STO/SnO_2 composite the activity increases by 22 folds. The activity can be further improved by the addition of H_2O_2 as an oxidant by 70 folds. This higher activity in presence of H_2O_2 can be due to the synergistic effect of photocatalysis, photosensitization and photo-Fenton process. The higher efficiency of H-(STO / SnO_2) composite sample along with H_2O_2 can also be accounted to the efficiency of non-radiative electron-transfer through Inter System Crossing (ISC) from the excited singlet to triplet state which increases the life time of the charge carriers. Triplet state is more favorable than the excited singlet state for the transfer of electrons from the hemin molecule to the conduction band of H-(STO / SnO_2) composite and in turn to the adsorbed oxygen molecule. The actual life time of singlet state is~10^{-9} s and the triplet state is~10^{-5} s. The process of electron trapping either by oxygen triplet or by Fe^{3+} ion in the hemin molecule (in the presence of H_2O_2) reduces the rate of recombination of photo generated charge carriers.

***Citation: *Gomathi Devi, L., Anitha, B.G. and Shyamala, R.* 2019.** "Photosensitization, photocatalysis and photo fenton reactions of hemin anchored $SRTIO_3$ / sno_2 composite for the degradation of rhodamine b: a comparative study with pristine $SrTiO_3$ and SnO_2", *International Journal of Current Research*, 11, (04), 3199-3205.

INTRODUCTION

STO is one of the most interesting photo catalyst for both water splitting reaction and photo degradation of organic pollutants because of its strong catalytic activity, non-toxicity, chemical stability, photochemical stability and good biological compatibility. STO is a bimetallic oxide possessing perovskite structure (Jinshu Wang, 2004; Tarawipa Puangpetch, 2008 and Gomathi Devi, 2018). SnO_2 is a wide band gap semiconductor and can absorb only UV light of shorter wavelength (Gomathi, 2018; Wang Cun, 2002 and Lin Xu, 2012). STO is usually coupled with other semiconductors of lower band gap which is a novel approach to achieve efficient charge separation. The coupling increases the life time of the charge carriers and enhances the charge transfer process especially at the interface. The excitation of one of the semiconductor can lead to the transfer of electrons into the lower lying conduction band (CB) of the second semiconductor. The hole formed in this process can accumulate in the valance band (VB) of first semiconductor. Hence excited electrons and holes are separated effectively leading to the enhanced photocatalytic activity. The interfacial charge transfer process can be considered as band gap engineering provided the metal oxides have compatible band gap structure. In the present case STO and SnO_2 when used individually possess two major drawbacks: i) both the materials require an excitation wavelength that falls in the UV region which hampers the exploitation of solar light in the photocatalytic reaction and ii) the rate of recombination of photogenerated charge carriers reduces the quantum efficiency of photocatalysis. Hence an attempt is made to incorporate these two materials in a composite and to focus on the charge transfer mechanism between them so that the above mentioned drawbacks can be overcome. Further an attempt is made to modify the metal oxide surfaces by the hemin which is an inorganic metal complex. Molecular modification of wide band gap metal oxide semiconductor is a field of high interest in heterogeneous catalysis/most of the reported studies in the literature are mainly concerned with semiconductor modification especially by highly conjugated organic dye molecules (Shendong Zhuang, 2014). The photosensitization by dyes, ruthenium polypyridyl complexes, porphyrins etc., have shown to be better technique for an excellent visible light harvesting with higher efficiency compared with other methods (Pan Zhang, 2010 and Andrea Maldotti, 2011). Inorganic metal complexes can act as photosensitizers in which a transition metal ion is bonded to either inorganic or organic ligands. These ligands are coordinately bond to the central metal ion. Inspired by the biological systems like photosynthesis, many different compounds like hemin can be used as a sensitizer which can mimic the naturally occurring

***Corresponding author:* Gomathi Devi, L.,**
Department of Post Graduate Studies in Chemistry, Central College City Campus, Dr. Ambedkar Street, Bangalore University, Bangalore 560001, India.

reactions due to its excellent oxidative capacity. Hemin is a class of macrocyclic compound with rigid conjugate structure. Hemin shows strong absorption in the 400-450 nm region which is referred to as Soret band and also in the 500-700 nm region which is called Q-band. Hemin possess excellent chromophoric activity over the entire region of solar spectrum and it possess good electron donating properties due to their large π electron system. One of the most significant techniques to obtain efficient selective and reusable catalyst is to immobilize metalloporphyrins on the catalyst surface. The extension of the absorption in the visible region is due to the extensive system of the delocalized π electrons. Hemin is known to be a good photosensitizer due to the excellent photophysical properties like high quantum yield for inter system crossing with small singlet−triplet splitting energy and long triplet state life time. Anchoring of the hemin on the surface of the $SrTiO_3$ / SnO_2 (STO/SnO_2) composite can be considered as hybrid of organic and inorganic counter parts with real excellent catalytic prospective.

MATERIALS AND METHODS

Tetra butyl titanate (97%) was obtained from Sigma Aldrich. Citric acid, strontium nitrate, ethanol (HPLC grade), Hemin, acetonitrile AR and Tin chloride ($SnCl_2.2H_2O$) and dimethyl sulfoxide and acetonitrile (DMSO) were obtained from Merck Chemicals Limited. Hydrogen peroxide (30%w/v) was obtained from Sisco-Chemical Industries. Ammonia, Rhodamine B (RhB) and dimethyl sulfoxide, were obtained from SD Fine Chemicals. Double distilled water was used throughout the experiment.

Preparation of STO, SnO_2 and STO/ SnO_2 composite: STO and SnO_2 were prepared by using the methods reported earlier. STO/ SnO_2 composite was prepared by mechano-chemical ball milling process. This process involves combining STO and SnO_2 in 1:1 ratio and subjecting it to the ball milling process in the reactor. During the process of ball milling 5-10 ml of water was added. The ball milling process was carried out for about 3 hours at a speed of 600 rpm. The obtained powder was dried at 110°C in an oven to obtain STO/ SnO_2 composite.

Preparation of H-(STO/ SnO_2) composite: Surface modification of STO/ SnO_2 composite by hemin was carried out by immersing 1 g of the composite catalyst in 5 μM hemin solution (Aruna Kumari, 2015). The solvent used is 1:1 mixture of dimethyl sulfoxide and acetonitrile ($DMSO/CH_3CN$). The catalyst was immersed in the hemin solution for 24 h. Further the catalyst particles were separated by the centrifugation method and the sample was dried at room temperature.

Characterization of the photo catalysts: The prepared samples were characterized by the following techniques. The powder X-ray diffraction (PXRD), Fourier transform infrared (FTIR) spectra, absorption spectra (DRS), scanning electron microscopic (SEM) technique, EDX analysis, Brunner–Emmet–Teller (BET) studies. The details pertaining to characterization process and the elaborate experimental procedures are mentioned in our previous reports (Gomathi; Bui, 2013). The residual concentration of the Rh B at different time intervals during the reaction process was monitored by the UV-visible absorption technique at 554 nm (λ_{max}). Electrical impedance (EIS) measurements were carried out in an electrochemical work station (CH Instruments model CH601E). The electrochemical cell consists of three electrodes. The working and the counter electrodes were made of Pt. The current / potential measurements were made with respect to Ag/AgCl standard electrode. The electrolytes used is a mixture of [K_3 Fe (CN_6)] and [K_4 Fe (CN_6)] in 0.5 M KCl solution. Working electrode was prepared by using graphite powder along with the appropriate amount of photo catalysts sample in the ratio of 80:20. Few drops of silica gel is used as a binder. The resulted paste is packed into the cavity of polypropylene tube (2.55 mm internal diameter and 5mm depth). Copper wire is used as an electrical contact.

RESULTS AND DISCUSSION

PXRD studies: PXRD patterns of STO, SnO_2, STO/ SnO_2 composite and H-(STO/ SnO_2) composite are given inFig.1 a & b).The peaks pertaining to STO can be represented by the following 2θ values of 32.35˚ (110), 39.91˚ (111), 46.42˚ (200), 57.72˚ (211), 67.74˚ (220) and 77.09˚ (310) (JCPDS card No: 74-1296). These 2θ peaks were observed distinctly in STO, STO/ SnO_2 composite and H-(STO/ SnO_2) composite samples. The peaks corresponding to SnO_2 were observed at 2θ values of 26.61˚ (110), 33.89˚ (101), 37.95˚ (200), 51.78˚ (211), 54.75˚ (220), 57.82˚ (002), 61.87˚ (310), 64.71˚ (112), 65.93˚ (301), 71.27˚ (202) and 78.71˚ (321) (JCPDS card of SnO_2, No. 41-1445). SnO_2, STO/ SnO_2 composite and H-(STO/ SnO_2) composite samples show these distinct peaks (the numbers in the parenthesis indicates the hkl values). From the PXRD pattern it could be concluded that there was no detectable change in the structure of either STO or SnO_2in both the composites. Anchoring of hemin on the surface of STO/ SnO_2 composite had not influenced any structural change. No characteristic peak corresponding to hemin was observed since the concentration of hemin was well below the PXRD detection limit. The PXRD results confirmed the existence of both STO and SnO_2 in the composite. Percentage composition of STO and SnO_2 in the STO/ SnO_2 composite is further confirmed by the qualitative analysis and the values were found to be 50 % for each of individual constituent respectively (Gomathi, 2018).

UV-Visible absorption spectral studies: The Fig.2 shows absorption spectra of STO, SnO_2, STO / SnO_2 composite and H-(STO / SnO_2) composite samples. STO exhibits a strong absorption band in the UV region corresponding to charge-transfer from the VB to CB at 389 nm. The band gap energy values were calculated by using the formula $E_g = 1240/\lambda$, where λ is the wavelength of maximum absorption of the catalyst. The optical absorption threshold for SnO_2, STO / SnO_2 composite and H-(STO / SnO_2) composite samples were observed at 344 nm, 395 nm and 436 nm corresponding to the band gap of 3.6 eV, 3.12 eV and 2.84 eV respectively. The hemin anchored sample shows red shift in the absorption towards the visible region. This extension in the absorption towards the visible region could be due to the delocalization of π-electrons in the porphyrin ring (Soret bands). The expansion of the Q-band region around 450-550 nm corresponds to the a_{2u} (π) to e_{g^*} (π) transition for H-(STO / SnO_2) composite. This prominent absorption confirms the presence of chemisorbed hemin molecules on the surface of STO / SnO_2 composite.

FTIR studies: FTIR spectra provide specific information about the molecular structure, chemical bonding and molecular environment (Fig. 3 a&b).

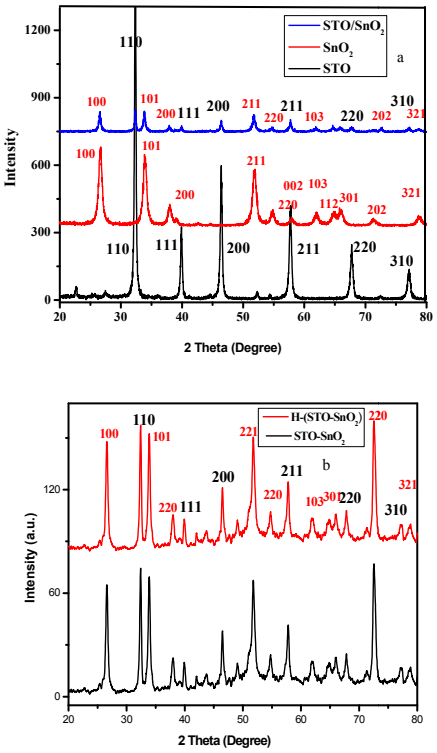

Fig. 1. PXRD patterns of (a) STO, SnO_2, STO/ SnO_2 composite and (b) STO/ SnO_2 composite and H-(STO/ SnO_2) composite

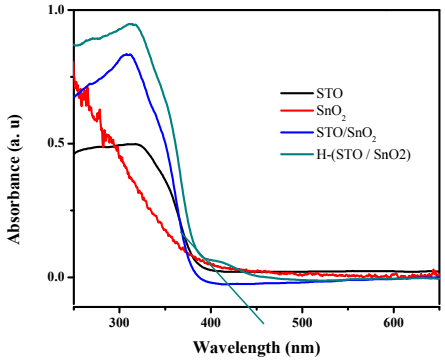

Fig. 2. UV-visible absorption spectra of STO, SnO_2, STO / SnO_2 composite and H-(STO / SnO_2) composite samples

The FTIR spectra of the hemin system can be better understood by considering its structure as shown in the scheme. 1 which shows the protoporphyrin (IX) ring system with Fe (III) occupying the center of its cavity along with a coordinated chloride ion. The Fe (III) center is square pyramidal in geometry, due to the high spin penta coordination of ligands. The porphyrin ring has several side chains like carboxyethyl, vinyl and methyl groups. Fig. 3 shows the FTIR spectra of STO, SnO_2, STO / SnO_2 composite and H-(STO / SnO_2) composite samples. STO shows characteristic band around 447 cm^{-1} and 537 cm^{-1} are corresponding to the bending and stretching vibration of Ti-O bonds in TiO_6 octahedron. SnO_2 shows peak splitting around 400 nm to 600 nm corresponding to the asymmetric and symmetric starching of Sn-O in Sn-O-Sn bond. In the case of STO / SnO_2 composite and H-STO / SnO_2 composite, these vibrations overlap with one another and speculation of such vibrations becomes rather difficult. The hemin anchored sample shows two characteristics broad bands around 3480-3600 cm^{-1} and 1640 cm^{-1} are ascribed to the stretching and bending modes of vibrations of chemisorbed and /or physisorbed H_2O molecule on the catalyst surface, which confirms the existence of Ti-OH vibration. Further, these peaks also confirm the presence of uncoordinated -COOH group and hydrogen bonded -COOH groups of adsorbed hemin molecule. The spectra of hemin anchored catalysts show an highly intense band at 1020 cm^{-1} due to the C-O stretching vibration and a split peak around 1450-1400 cm^{-1} corresponding to C=O vibrations of surface bound carboxylic acid and hydrogen bonded carboxylic acid respectively. FTIR study confirms the binding of hemin molecule to the metal oxide surface through O=C-O-Ti bond.

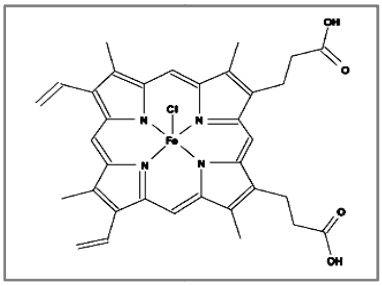

Scheme. 1. Structure of hemin

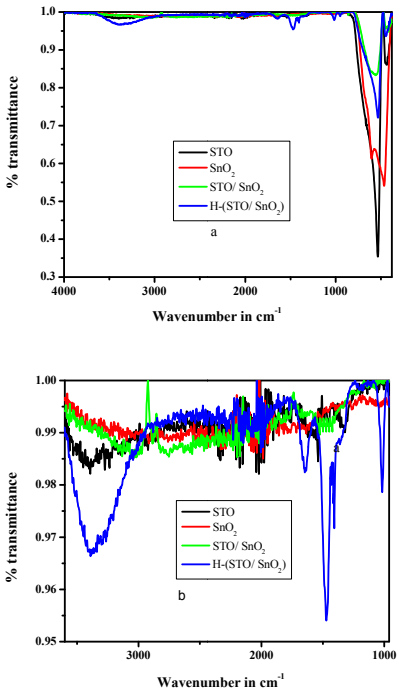

Fig. 3. The FTIR spectra of STO, SnO_2, STO/SnO_2 composite and H-(STO/SnO_2) composite samples

SEM analysis: The surface morphology of all the samples were studied from the SEM images (Fig. 4). The morphology of the unmodified catalysts were found to be spherical and the composites show agglomeration. The morphology of H-(STO / SnO_2) composite sample is very much similar to the STO / SnO_2 composite. EDX technique was used to determine the composition of H-(STO / SnO_2) composite which shows the presence of all the elements Sr, Ti, Sn, O, Fe, N, C and Cl (Fig. 5) and Table.1 shows the weight percentages of respective elements in H-(STO / SnO_2) composite sample.

XPS studies: XPS technique is used to obtain more detailed information on the chemical state of ions in the H-(STO / SnO_2) composite sample (Fig. 6). XPS spectra of O 1s shows two BE peaks at 529.6 eV and 532.2 eV for oxygen linked with Sr / Ti or Sn metal ion and the oxygen bonded to hydroxyl ion respectively.

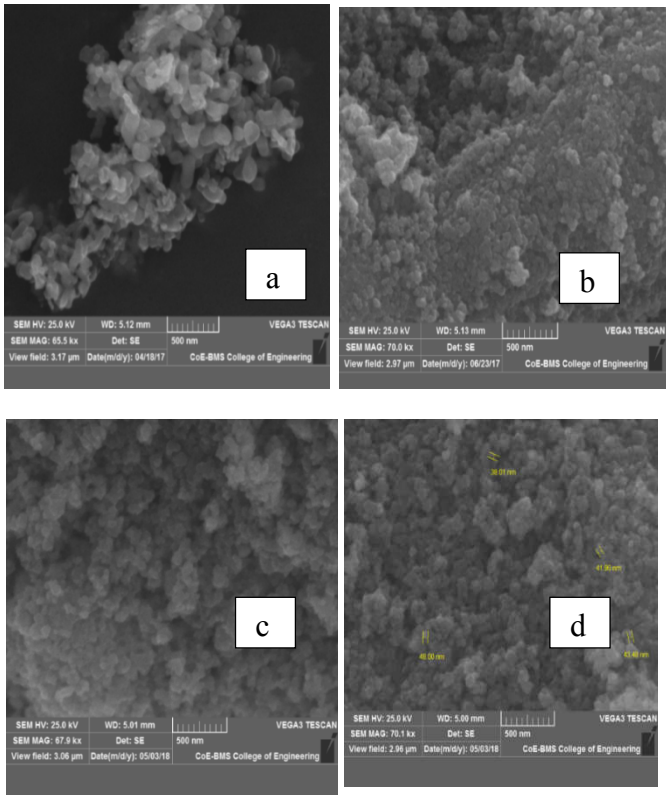

Fig. 4. SEM images of (a) STO, (b) SnO_2 (c) STO / SnO_2 composite and (d) H-(STO / SnO_2) composite samples.

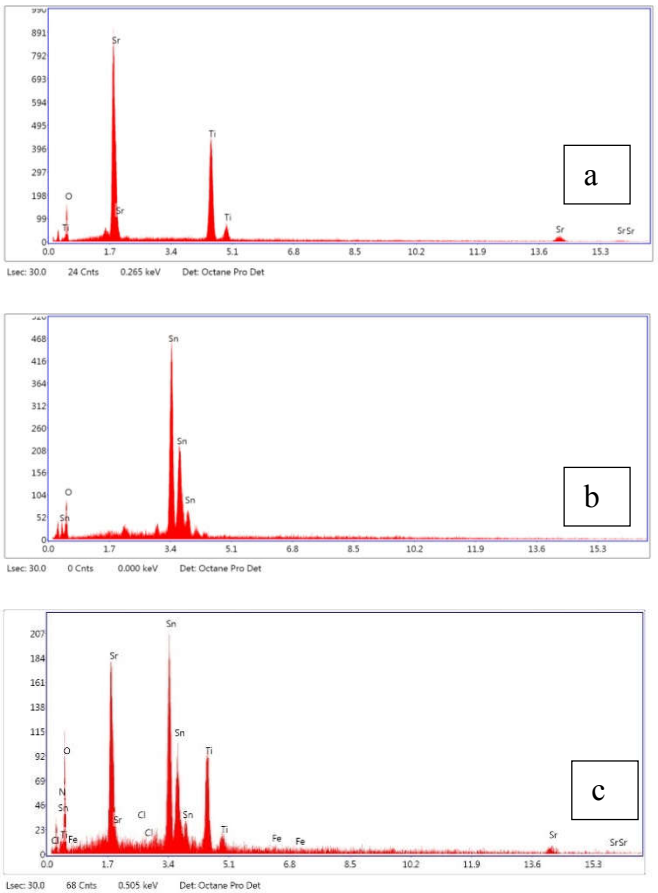

Fig. 5. EDX spectra of (a) STO, (b) SnO_2 and (c) H-(STO / SnO_2) composite samples.

C1s spectrum shows the five distinct peaks corresponding to 284.4 eV (C–C), 285.8 eV (C–N), 286.4 eV (C–O), 288.6 eV (C=O) and 288.79 eV (O–C=O). N 1s spectrum shows a single BE peak at 399.3 eV corresponding to the four chemically equivalent N atoms which are bound to the central Fe atom in the porphyrin ring. The XPS spectrum of Fe 2p has three BE peaks at 709.75 eV (Fe 2 p $_{3/2}$), 714.37 eV (Fe 2 p 1/2), and a satellite peak at 712.28 eV. The BE peaks of Fe 2 p $_{3/2}$ are usually expected to be found between 710.6 and 711.2 eV. The shift observed in the present case is due to the strong interaction. Similarly N 1s BE peak is expected at 401.8 eV. But in the present case the BE peak is shifted by ~1.5 eV suggests a strong interaction of hemin molecule with STO /SnO_2 composite.

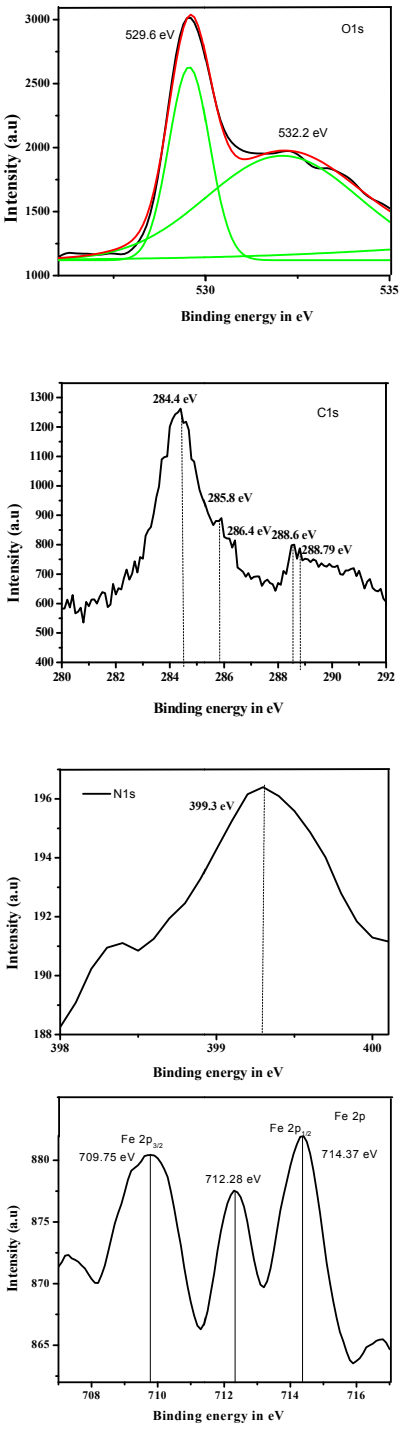

Fig. 6. High resolution XPS spectra of O1s, C1s, N1s and Fe 2p spectrum of H-(STO / SnO_2) composite sample.

Electrical Impedance study (EIS): Electrical impedance spectroscopy is an effective technique for probing the resistance offered by the material for the conduction of current. The magnitude of the arc radius determines the resistivity

offered by the catalyst system. Smaller the arc radius higher will be the charge transfer efficiency and vice versa. EIS of all the samples are shown in Fig. 7. H-(STO / SnO_2) composite sample shows lowest radius compared to all the other samples. STO and SnO_2 show almost similar high resistivity. The resistivity of the STO / SnO_2 composite is less than the STO and SnO_2 samples and it is higher than the H-(STO/SnO_2) composite.

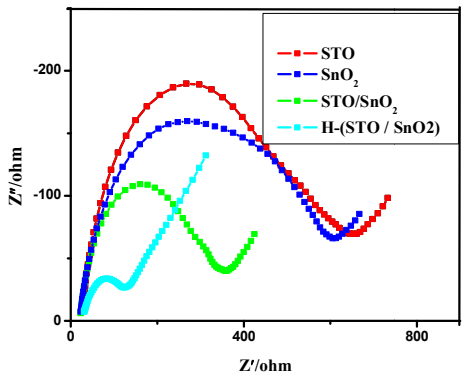

Fig. 7 Electrical Impendence spectra of STO, SnO_2, STO / SnO_2 composite and H-(STO / SnO_2) composite samples

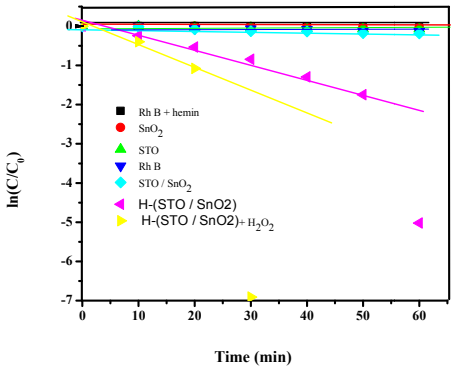

Fig. 8 plot of ln C/C_0 versus time in minutes for the degradation of RhB

Photocatalytic activity: The photocatalytic activity of STO, SnO_2, STO / SnO_2 composite and H-(STO / SnO_2) composite samples were evaluated for degradation of RhB under the solar light irradiation. The activity of STO and SnO_2 was very poor due to their higher band gaps. STO / SnO_2 composite showed only 16 % degradation under the illumination of solar light with the rate constant values of 0.133×10^{-2} min^{-1} and 0.081×10^{-2} min^{-1} respectively. H-(STO/SnO_2) composite showed 99 % degradation in 60 min time duration with rate constant value of 6.72×10^{-2} min^{-1} due to the photosensitization process by hemin molecule. Further the degradation reaction using H-(STO / SnO_2) composite was carried out in the presence of an oxidant like H_2O_2. This reaction showed remarkable increase in the reaction rate and the degradation was completed within 30 min with a rate constant value of 21.408×10^{-2} min^{-1}. Fig. 8 shows the extent of degradation of RhB versus irradiation time for all the four mentioned catalysts systems. The photocatalytic activity shows the following increasing order: RhB + hemin <SnO_2 < STO < RhB < STO / SnO_2<H-(STO / SnO_2) < H-(STO / SnO_2) composite + H_2O_2. The plot of ln C/C_0 versus time in minute gives a straight line with negative slope which is equal to –k, which demonstrates that the reaction was found to follow approximately first order kinetics (Fig. 8). C_0 and C are the concentration of RhB at time zero and at time t and k is the reaction rate constant.

Results shows that the RhB itself can absorb solar light and self-destruction takes place which shows that 11 % degradation in 60 min. Further the reaction in which both RhB and hemin are taken, the degradation efficiency was reduced to 4%. This can be due to the recombination of photo generated electrons migrated from RhB to hemin due to the staggering of HOMO and LUMO energy levels of both these molecules (Shendong Zhuang, 2014 and Pan Zhang, 2010). The enhanced activity of H-(STO / SnO_2) composite along with the H_2O_2 oxidant can be attributed to: i) photosensitization by both hemin and RhB molecules; ii) occurrence of photo Fenton type of reactions due to the presence of H_2O_2 and Fe which exists in multiple oxidation states (Fe^{2+} and Fe^{3+}); iii) suitable band edge positions of composite with respect to hemin and RhB and iv) efficient separation of photoinduced electron hole pairs. The photocatalytic degradation reaction can proceed in two different ways: i) photoexcitation of electrons from VB to the CB due to the mixing up of energy levels of STO and SnO_2 and ii) photosensitization by hemin or RhB molecule where anelectron is excited from highest occupied molecular orbital (HOMO) to lowest unoccupied molecular orbital (LUMO). This electron further moves into the CB of either STO or SnO_2 semiconductor. The percentage degradation and rate constant values of all the experiments are given Table 1.

Table 1. Type of catalyst, duration of the reaction time period, % degradation and the rate constant values for STO, SnO_2, STO / SnO_2 composite and H-(STO / SnO_2) composite samples for the degradation of RhB

Reaction	Time in min	% degradation	$k \times 10^{-2}$ (min^{-1})
RhB + hemin	60	3.5	0.072
SnO_2	60	4	0.08
STO	60	6	0.13
RhB	60	11	0.22
STO/SnO_2	60	16	0.33
H-(STO / SnO_2)	60	99	6.72
H-(STO / SnO_2)+H_2O_2	30	99.9	21.4

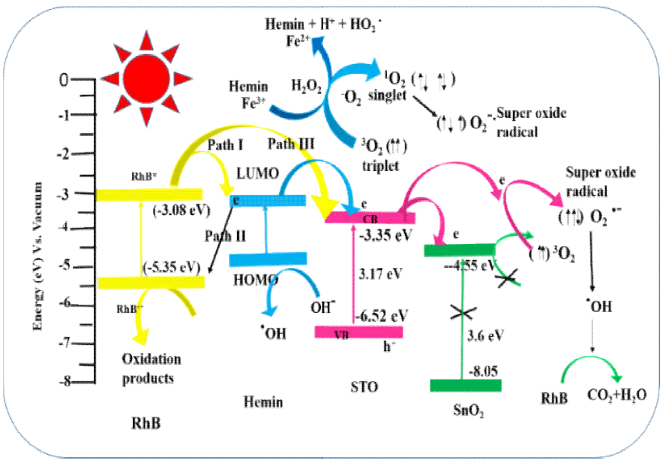

Scheme 2: Electronic energy levels of RhB, hemin, STO / SnO_2 composite with respect to vacuum representing various electronic transitions and interfacial charge transfer process depicting the generation of highly active singlet oxygen ($^1O_2$ ↑↓ ↑↓) from less active triplet oxygen $^3O_2$ (↑↑).

The stepwise vectorial electron transfer takes place in the following way (Scheme 2): i) from the LUMO of RhB to LUMO of hemin (path I); ii) from LUMO of hemin to HOMO of RhB showing recombination of photogenerated charge carriers (path II); iii) from the LUMO of RhB / hemin to the CB of STO / SnO_2composite (path III). The excitation of RhB can be expressed in the following way:

$$RhB + h\upsilon \xrightarrow{\text{visible light}} RhB^* \quad \text{Excitation of dye} \quad (8.1)$$

$$RhB^* + H\text{-}(STO/SnO_2) \rightarrow RhB^{\bullet+} + H\text{-}(STO/SnO_2)(^-e_{CB}) \quad \text{Electron injection via hemin/directly} \quad (8.2)$$

Hemin [H] can be activated from its ground state to excited singlet state ^{1}[H]* through one photon absorption under visible light. The λ_{max} of hemin can be observed in the visible light region due to the presence of extensive conjugation system along with its delocalized π electrons. These excited singlet states could be relaxed to the lowest excited triplet state ^{3}[H]* through non-radiative Inter System Crossing (ISC) path way [11]. The life time of singlet state is quite shorter ~10^{-9} s than the life time of the triplet excited state~ 10^{-5} s, which gives enough time for the subsequent transfer of excited electrons to the CB of STO or SnO_2 in the H-(STO / SnO_2) composite, since the LUMO of hemin molecule is situated above the CB of STO [11]. The band edge positions of STO and SnO_2 in the composite can be found by using the following formulae:

$$E_{CB} = \chi - E^e - 0.5E_g$$

$$E_{VB} = E_{CB} + E_g$$

Where, E_{CB} and E_{VB} are the CB and VB edge potentials, χ is the absolute electro negativity of the semiconductor, which is the geometric mean of the electro negativity of the constituent atoms. E_e is the energy of free electrons on the hydrogen scale (4.5 eV), E_g is the band gap energy of the semiconductor. E_{CB} and E_{VB} of STO were determined to be −1.145 and 2.025 eV, while those of SnO_2 are positioned at -0.05 and 3.55 eV vs. NHE (normal hydrogen electrode) respectively. E_{CB} of SnO_2 lies below the E_{CB} of STO thus, the electrons captured in the CB of STO would smoothly transfer to the CB of SnO_2 in the composite. The electrons in the CB of SnO_2 cannot react with molecular O_2 to produce $^{\bullet}O^{2-}$ radicals because of unsuitable band edge positions. But the electrons in the CB of STO could react with molecular O_2 to produce $O^{2\bullet-}$ and radicals. These $O^{2\bullet-}$ in turn reacts with water to give peroxo radical ($HOO^{\bullet}$), which ultimately give rise to highly active $^{\bullet}OH$ radicals. On the other hand the holes in the VB of hemin can react with water molecule or hydroxyl anion to produce hydroxyl free radicals. Thus, the recombination of photogene rated electrons and holes could be quenched to the maximum extent, which in turn facilitates the photo catalytic degradation of RhB dye. The various proposed reaction path ways can be summarized as follows:

$$[H] + h\upsilon \xrightarrow{\text{visible light}} {}^1[H]^* \;\; \xrightarrow{\text{Non-radiative ISC}} {}^3[H]^* \quad \text{Excitation of hemin} \quad (8.3)$$

$$^{1 \text{ or } 3}[H]^* \rightarrow H^+ + e \quad (8.4)$$

$$e + H\text{-}(STO/SnO_2) \rightarrow H\text{-}(STO/SnO_2)(^-e_{CB}) \quad \text{Electron transfer from hemin} \quad (8.5)$$

$$H\text{-}(STO/SnO_2)(^-e_{CB}) + O_2 \rightarrow O_2^{\bullet-} + H\text{-}(STO/SnO_2)^+ \quad \text{Electron trapping by molecular oxgen} \quad (8.6)$$

$$H\text{-}(STO/SnO_2)(^-e_{CB}) + O_2^{\bullet-} + H^+ \rightarrow H\text{-}(STO/SnO_2) + HOO^{\bullet} \quad (8.7)$$

$$HOO^{\bullet} + H^+ \rightarrow H_2O_2 \quad (8.8)$$

$$H_2O_2 + e_{CB} \rightarrow HO^{\bullet} + OH^- \quad (8.9)$$

$$H\text{-}(STO/SnO_2)^+ + OH^- \rightarrow H\text{-}(STO/SnO_2) + HO^{\bullet} \quad (8.10)$$

$$RhB^{\bullet+} / RhB + O_2^{\bullet-} \rightarrow\rightarrow CO_2 + H_2O_2 \quad \text{Minerlization process} \quad (8.11)$$

$$RhB^{\bullet+} / RhB + HO^{\bullet} \rightarrow\rightarrow CO_2 + H_2O_2 \quad \text{Minerlization process} \quad (8.12)$$

The possibility of formation of highly active singlet oxygen in the case of porphyrins is confirmed by the previous study. Formation of singlet oxygen [$^1O_2$] is possible by the electron transfer from the LUMO of hemin molecule directly to the triplet state of oxygen or by two step electron transfer process i) electron transfer from the LUMO of the hemin molecule to the CB of STO and ii) electron transfer from the CB of STO to the triplet oxygen state. Singlet oxygen [$^1O_2$] can enhance the rate of oxidation of pollutant RhB molecule. In addition to this, upon addition of H_2O_2 as a strong electron acceptor the rate of the reaction is enhanced by 4 folds for H-(STO / SnO_2) composite with a rate constant 21.408 × 10^{-2} min^{-1}. There is a remarkable enhancement in the rate of photocatalytic degradation due to the continuous cyclic process in which Fe^{3+} ion of hemin reacts with H_2O_2 to generate Fe^{2+} ion and peroxo radical ($HOO^{\cdot}$) and this free radical in turn can react with Fe^{2+} ion in presence of H^+ ions to regenerate Fe^{3+} ion and H_2O_2. The H_2O_2 can act as an electron acceptor and traps the photo generated electrons. Hopping of electron between Fe^{2+} and Fe^{3+}oxidation states is common in the photo-Fenton type of process. When Fe^{3+} accepts the electron its stability is lost and this type of trapping is called as shallow trapping.

$$H_2O_2 + Fe^{3+} \rightarrow Fe^{2+} + HO_2^{\bullet} + H^+ \quad (8.13)$$

$$Fe^{2+} + HO_2^{\bullet} \rightarrow Fe^{3+} + H_2O_2 \quad (8.14)$$

$$H_2O_2 + O_2^{\bullet-} \rightarrow HO^{\bullet} + HO^- + O_2 \quad (8.15)$$

Conclusion

STO and SnO_2 are wide band gap metal oxide semiconductors which shows activity only under UV-light. But when these two semiconductor materials are coupled with one another in a composite, they show activity under visible light due to the staggering of band edge positions. However the activity under solar light irradiation is very low due to the higher extent of recombination of photogenerated charge carriers. Photosensitization process dominates when hemin is anchored on the STO/SnO_2 composite. The synergistic effect between photo catalysis and photo Fenton process increases the activity of H-(STO/SnO_2) composite in presence of H_2O_2 as an oxidant and the reaction rate increases by 70 folds. The higher efficiency of H-(STO/SnO_2) composite sample along with H_2O_2 can also be accounted to the efficiency of non-radiative electron-transfer process through ISC from excited singlet to triplet state increasing the life time of the charge carriers. Triplet state is more favorable than the excited singlet state for the transfer of photo generated electrons from the hemin molecule to the CB of H-(STO / SnO_2) composite. These electrons in turn are transferred to the adsorbed oxygen molecule. The limiting parameter in all the reactivity studies is the life time of a particular state. The actual life time of singlet state is~10^{-9} s and the triplet state is~10^{-5} s. A short lived state of high reactivity can be less efficient in the reaction than a long lived state of lower reactivity. The process of electron trapping either by oxygen triplet or by Fe^{3+} ion in the hemin molecule (in the presence of H_2O_2) reduces the recombination of photo generated charge carriers to a greater extent.

Funding: University grants commission, Government of India for DSA-SAP program.

Conflict of interest: There are no conflict of interest.

REFERENCES

Martı´nez-de la Cruz A., U.M. Garcı´a Pe´ rez. 2010. “Rapid Mineralization of Rhodamine B Wastewater by Microwave Synergistic Fenton-Like Oxidation Process” Mater. Res. Bull. 45: 135-141.

A. Martínez-de la Cruz, S.M.G. Marcos Villarreal, Leticia M. Torres-Martínez, E. López Cuéllar, U. Ortiz Méndez. 2008. “Photoassisted degradation of rhodamine B by

nanoparticles of α-$Bi_2Mo_3O_{12}$ prepared by an amorphous complex precursor" Mater. Chem. Phys.112:679-685.

Andrea Maldotti, Leonardo Andreotti, Alessandra Molinari, Sergey Borisov, and Victor Vasil ev. 2001. "Photoinitiated Catalysis in Nafion Membranes Containing Palladium(II) meso□Tetrakis(N□methyl□4□pyridyl)porphyrin and Iron (III) meso□Tetrakis(2,6□dichlorophenyl)porphyrin for O_2 Mediated Oxidations of Alkenes" Chem. Eur. J. 7:16.

D-N Bui, Jin Mu, Lei Wang, Shi-Zhao Kang, Xiangqing Li. 2013. "Preparation of Cu-loaded $SrTiO_3$ nanoparticles and their photocatalytic activity for hydrogen evolution from methanol aqueous solution" Appl. Surf. Sci. 274: 328-333.

Hongbo Fu, Chengshi Pan, Wenqing Yao, and Yongfa Zhu. 2005. "Visible-Light-Induced Degradation of Rhodamine B by Nanosized Bi_2WO_6" J. Phys. Chem. B 109:2432-22439.

Humaira Seema, K. C. Kemp, Vimlesh Chandra and K. S. Kim. 2012. "Graphene–SnO_2 composites for highly efficient photocatalytic degradation of methylene blue under sunlight Nanotechnology 23:355705.

Jianting Tang, Datang Li, Zhaoxia Feng, Zhen Tan and Baoli Ou. 2014. "A novel AgIO4 semiconductor with ultrahigh activity in photodegradation of organic dyes: insights into the photosensitization mechanism" RSC Adv., 4: 2151-2154.

Jinshu Wang, Shu Yin, Masakazu Komatsu, Qiwu Zhang, Fumio Saito, Tsugio Sato. 2004. "Photo-oxidation properties of nitrogen doped $SrTiO_3$ made by mechanical activation" *Appl. Catal.,* B: Environ. 52:11-21.

K. Yang, B. Xing. 2010. "Adsorption of Organic Compounds by Carbon Nanomaterials in Aqueous Phase: Polanyi Theory and Its Application" Chem. Rev. 110:5989-6008.

L. Gomathi Devi and R. Shyamala. 2018. "Photocatalytic activity of SnO_2–α-Fe_2O_3 composite mixtures: exploration of number of active sites, turnover number and turnover frequency" Mater Chem. Front., 2:796.

L. Gomathi Devi, B.G. Anitha.2018. "Exploration of vectorial charge transfer mechanism in TiO_2/$SrTiO_3$ composite under UV light illumination for the degradation of 4-Nitrophenol: A comparative study with TiO_2 and $SrTiO_3$" Surf. Interface, 11:48-56.

Lin Xu, Ellen M. P. Steinmiller, and Sara E. Skrabalak. 2012. "Achieving Synergy with a Potential Photocatalytic Z-Scheme:Synthesis and Evaluation of Nitrogen-Doped TiO_2/SnO_2 Composites" J. Phys. Chem. C 116:87-877.

M. L. ArunaKumari and L. Gomathi Devi. 2015. "New insights into the origin of the visible light photocatalytic activity of Fe(III) porphyrin surface anchored TiO_2" Environ. Sci. Water Res. Technol. 1:177-187.

Pan Zhang, Mei Wang, Caixia Li, Xueqiang Li, Jingfeng Donga and Licheng Sun. 2010. "Photochemical H_2 production with noble-metal-free molecular devices comprising a porphyrin photosensitizer and a cobaloxime catalyst" Chem. Commun., 46:8806-8808.

Shendong Zhuang, Xiaoyong Xu, Bing Feng, Jingguo Hu, Yaru Pang, Gang Zhou, Ling Tong, and Yuxue Zhou. 2014. "Photogenerated Carriers Transfer in Dye–Graphene–SnO_2 Composites for Highly Efficient Visible-Light Photocatalysis" Appl. Mater. Interfaces, 6:613-621.

Shendong Zhuang, Xiaoyong Xu, Bing Feng, Jingguo Hu, Yaru Pang, Gang Zhou, Ling Tong, and Yuxue Zhou. 2014. "Photogenerated Carriers Transfer in Dye–Graphene–SnO_2 Composites for Highly Efficient Visible-Light Photocatalysis" Appl. Mater. Interfaces 6: 613-621.

Tarawipa Puangpetch, Thammanoon Sreethawong, Susumu Yoshikawa, Sumaeth havadej. 2008. "Synthesis and photocatalytic activity in methyl orange degradation of mesoporous-assembled $SrTiO_3$ nanocrystals prepared by sol–gel method with the aid of structure-directing surfactant" J. Mol. Catal. A: Chem. 287: 70-79.

Wang Cun, Zhao Jincai, Wang Xinming, Mai Bixian, Sheng Guoying, Peng Ping'an, Fu Jiamo. 2002. "Preparation, characterization and photocatalytic activity of nano-sized ZnO/SnO_2 coupled photocatalysts" Appl. Catal., B: Environ. 39:269-279.

Yong Xu and Martin A.A. Schoonen. 2000. "The absolute energy positions of conduction and valence bands of selected semiconducting minerals"Am. Mineral. 85: 543-556.

****